Monografías de la Real Academia de Ciencias de Zaragoza. **28:** 85–94, (2006).

Painting chaos: $\text{OFLI}^2_{\text{TT}}$

R. Barrio

Grupo de Mecánica Espacial. Dpto. Matemática Aplicada

Universidad de Zaragoza. 50009 Zaragoza. Spain.

Abstract

In this paper we review briefly a recently developed chaos indicator: the $\text{OFLI}^2_{\text{TT}}$, or more friendly the OFLI2. Using this new indicator we present several sensitivity plots for several classical problems: the Hénon-Heiles Hamiltonian system and an Extensible Pendulum.

Keywords: Chaos indicators, $\text{OFLI}^2_{\text{TT}}$, Taylor method

1 Introduction

When we intend to analyze the behavior of a dynamical system one of the most interesting questions is if it is possible to know if a given initial condition generates a chaotic orbit or not. Obviously, a first question is to answer what is chaos? In the literature there are several definitions. In physics and applied sciences people uses a notion of chaos that captures the notion of non-mensurability and adopt as definition the sensitive dependence on initial conditions. To prove that a system has mathematical chaos in a rigorous way cannot be done without a carefully theoretical study of the particular problem. Therefore, this has been done only for some important problems [11]. Thus, a numerical evidence of the behavior of a dynamical system has become an invaluable tool in the analysis of a problem. One of the most popular techniques is the computation of Poincaré Surfaces of Section (PSS), which allow us to distinguish regular from chaotic orbits. This technique was introduced by Poincaré and first used numerically to obtain sections of non-integrable systems by Hénon and Heiles [13]. However, the Poincaré sections are useful only for systems of two-degrees of freedom.

The last few years a large number of numerical techniques to detect chaos have appeared, as the Frequency Map Analysis [15, 16], the Heliticity and Twist Angles [7, 8], the Mean Exponential Growth factor of Nearby Orbits (MEGNO) [6], the Smaller ALigment Index (SALI) [17, 18] and the Fast Lyapunov Indicator (FLI) [9, 10]. Most of the researchers has focus their attention to the physical definition of chaos and they try to study the sensitivity to initial conditions by using the first order variational equations.

Obviously, these techniques do no provide a rigorous proof of chaos but they point out where is probable to have chaotic or regular conditions.

2 A Chaos Indicator based on second order variational equations: $\mathbf{OFLI}^2_{\mathrm{TT}}$

Most of the methods based on the first order variational equations have a drawback: how to choose the initial conditions of the variational equations? Note that asymptotically most of the indicators do not depend on the initial conditions of the variational equations but we are using these techniques at a short finite time and so some dependency may be found. Therefore, an indicator will show the dynamical behavior more easily for a set of initial conditions than for another one at the same final time. So, for a global picture based on an indicator we have to choose carefully our initial conditions. This fact motivated the extension of the OFLI indicator given in [2] where the $\mathrm{OFLI}^2_{\mathrm{TT}}$ or OFLI2 indicator at the final time t_f was defined as

$$\mathrm{OFLI}^2_{\mathrm{TT}} := \sup_{t_0<t<t_f} \log \|\{\delta \boldsymbol{y}(t) + \frac{1}{2}\,\delta^2 \boldsymbol{y}(t)\}^{\perp}\|, \tag{1}$$

where $\delta \boldsymbol{y}$ and $\delta^2 \boldsymbol{y}$ are the first and second order sensitivities with respect to carefully chosen initial vectors. In this case the variational equations up to second order and the initial conditions are

$$\begin{aligned}
\frac{d\boldsymbol{y}}{dt} &= \boldsymbol{f}(t,\boldsymbol{y}), & \boldsymbol{y}(t_0) &= \boldsymbol{y}_0,\\
\frac{d\,\delta\boldsymbol{y}}{dt} &= \frac{\partial \boldsymbol{f}(t,\boldsymbol{y})}{\partial \boldsymbol{y}}\,\delta\boldsymbol{y}, & \delta\boldsymbol{y}(t_0) = \boldsymbol{T}_0 &:= \frac{\boldsymbol{f}(t_0,\boldsymbol{y}_0)}{\|\boldsymbol{f}(t_0,\boldsymbol{y}_0)\|},\\
\frac{d\,\delta^2\boldsymbol{y}}{dt} &= \frac{\partial \mathbf{f}}{\partial \boldsymbol{y}}\,\delta^2\boldsymbol{y} + \frac{\partial^2 \mathbf{f}}{\partial \boldsymbol{y}^2}\,(\delta\boldsymbol{y})^2\,, & \delta^2\boldsymbol{y}(t_0) &= \mathbf{0},
\end{aligned} \tag{2}$$

where we have to understand the equations in a componentwise manner. Note that the vector $\boldsymbol{T}_0$ is the initial tangent vector to the flow.

The FLI and $\mathrm{OFLI}^2_{\mathrm{TT}}$ behave linearly for initial conditions on a KAM tori and on a regular resonant motion (but with different rate of growing), tend to a constant value for the periodic orbits and grow exponentially for chaotic orbits [2, 12].

Another remark is that the definition of Eqns. (1) and (2) gives us the value of the $\mathrm{OFLI}^2_{\mathrm{TT}}$ for a particular orbit for a given initial conditions. Where the indicator plays a more important role is not analysing just one orbit but a global set of initial conditions. That is, we select a two dimensional manifold of initial conditions or of parameters of the problem and we compute the $\mathrm{OFLI}^2_{\mathrm{TT}}$ for all of them. Now, the $\mathrm{OFLI}^2_{\mathrm{TT}}$ picture will describes us quite well the global dynamical properties of the system. We remark that the two dimensional manifold is a manifold of initial conditions or parameters and we not look for any crossing of the orbits as the classical PSS method does.

The $\text{OFLI}^2_{\text{TT}}$ Chaos Indicator is defined by using the second order variational equations. Therefore, in order to avoid the explicit generation of such a variational equations we have devised [3] an alternative that permits us to obtain the solution of the variational equations without computing them explicitly. This method is based on the classical Taylor method for the numerical solution of ODE [1, 4] and permits a direct calculation of any order sensitivity, in particular the solution of the second order variational equations.

3 Some $\text{OFLI}^2_{\text{TT}}$ plots

In this section we present some $\text{OFLI}^2_{\text{TT}}$ plots for several classical problems.

All the tests have been done in a standard personal computer, a PC Intel Pentium IV 2.8 GHz under Windows XP and using `g77` as programming language (a GNU `fortran77`). The $\text{OFLI}^2_{\text{TT}}$ pictures are generated for a regular grid of 1000×1000 initial conditions. The Poincaré sections, done for comparison, have been calculated using a symplectic and symmetric composition method given in GniCodes [14].

From now on, in all the $\text{OFLI}^2_{\text{TT}}$ pictures the white color is associated with a chaotical behavior and the black with periodic or highly regular orbits, intermediate gray values are associated with evolution from regular to chaotic orbits.

The first classical problem is the well known two degrees of freedom Hénon-Heiles system [13] given by the Hamiltonian

$$\mathcal{H}(x, y, X, Y) = \frac{1}{2}\left(X^2 + Y^2 + x^2 + y^2\right) + x^2\, y - \frac{1}{3} y^3,$$

and so the differential system is

$$\begin{aligned} \dot{x} &= X, \qquad & \dot{X} &= -x - 2x\, y, \\ \dot{y} &= Y, \qquad & \dot{Y} &= -y - x^2 + y^2. \end{aligned}$$

These equations model the motion of stars around a galactic center, assuming the motion restricted to the (x, y) plane and they where introduced in the context of analyzing if there exists two or three constants of motion in the galactic dynamics. On Fig. 1 we show the $\text{OFLI}^2_{\text{TT}}$ pictures on the y vs Y plane for $x = 0$ and X obtained from the constant value of the energy $E = \mathcal{H}$ ($E = 1/12$, 0.105, 1/8, 0.14865 and 1/6 for pictures A, B, C, D and E respectively). The final time considered is $t_f = 300$. The pictures A, C and E are obtained for values of the energy close to the ones given in the seminal paper of Hénon-Heiles [13] using Poincaré sections. As this system has been studied with a great detail for a large number of researchers we present it just for illustration of the behavior of the $\text{OFLI}^2_{\text{TT}}$ on this system. First, we observe as when the energy is low most of the orbits are regular as predicts the KAM theory. The chaotic zone begins to grow (B) and several chains of islands appear. Increasing the value of the energy the chaotic sea

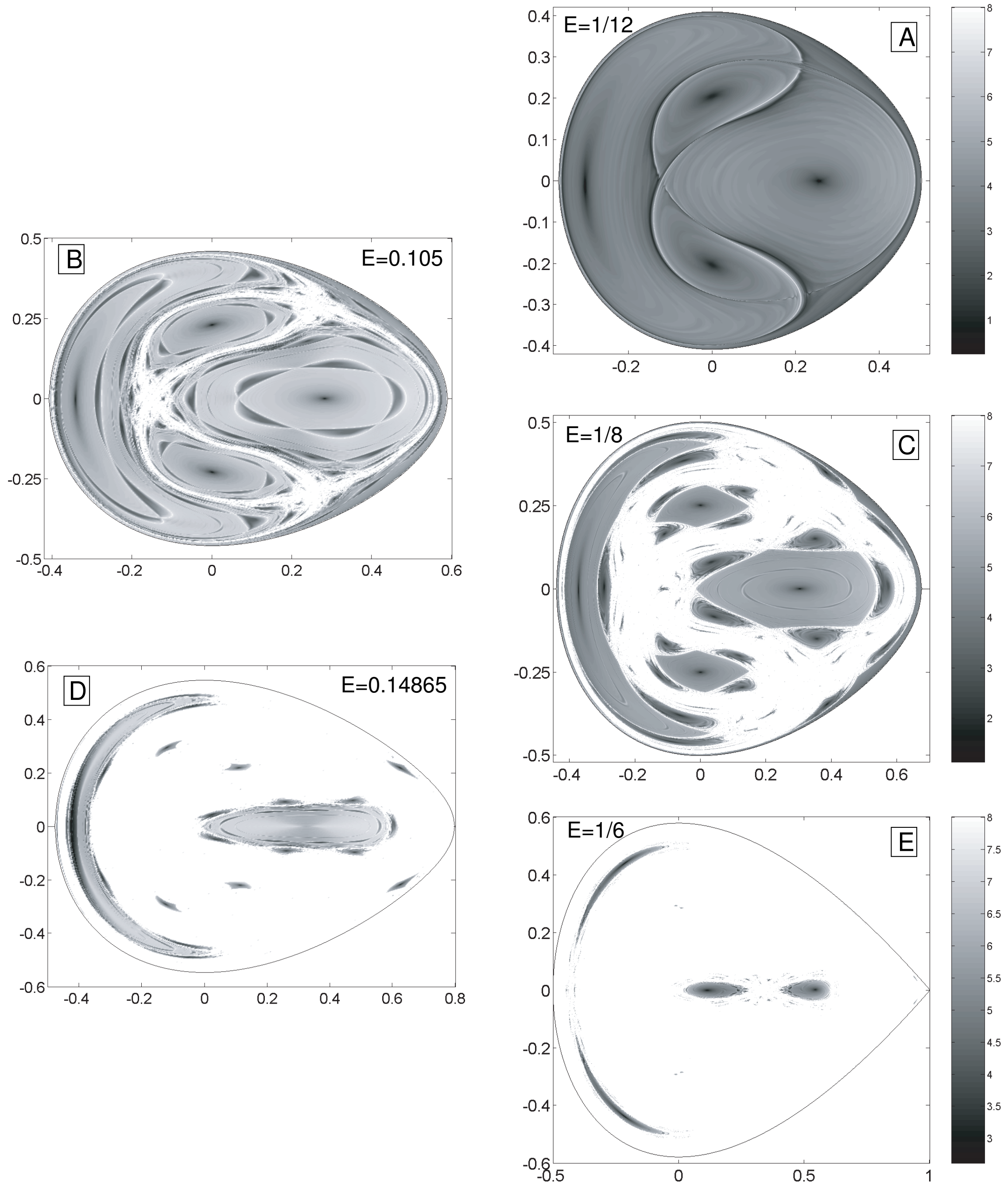

Figure 1: $\mathrm{OFLI}^2_{\mathrm{TT}}$ pictures for several values of the energy for the Hénon-Heiles system.

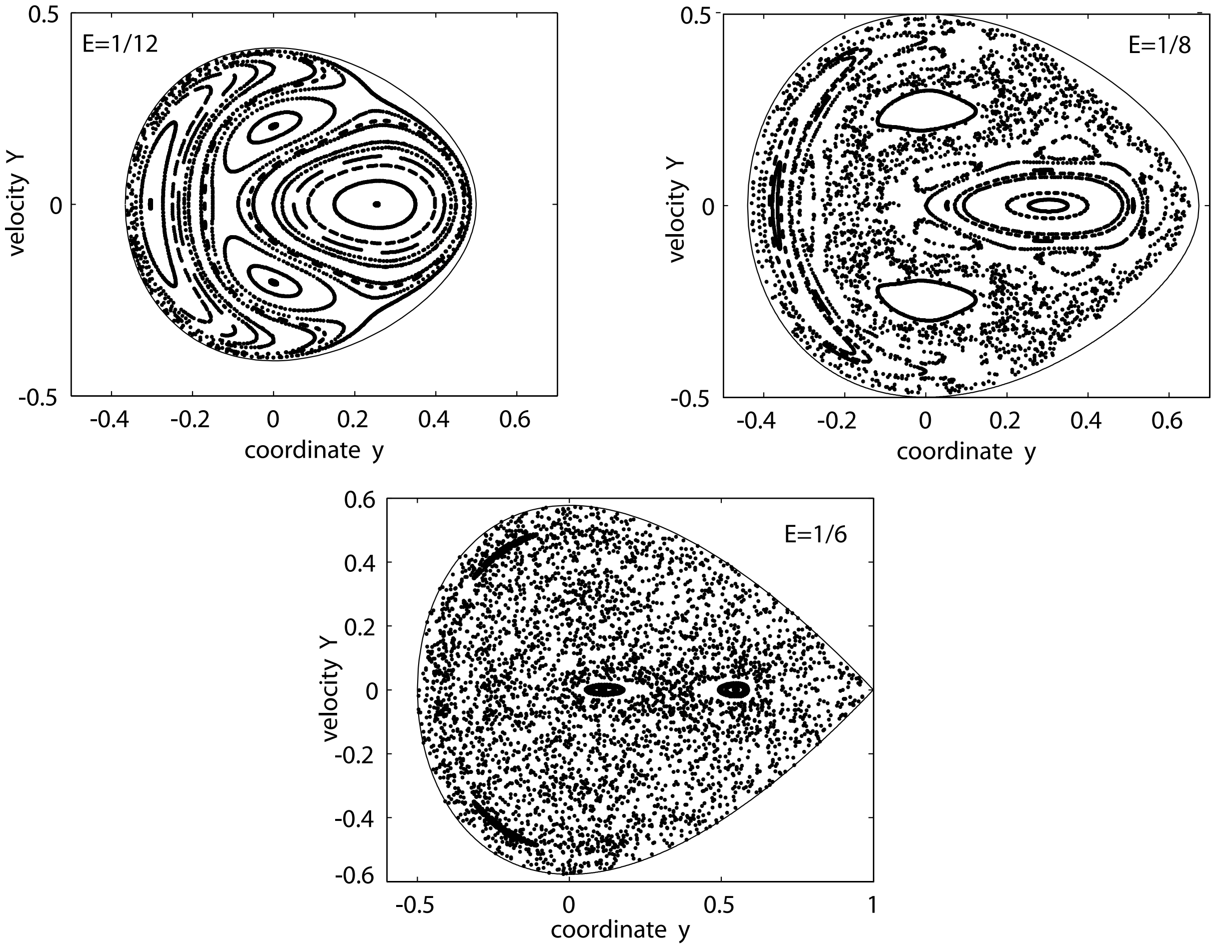

Figure 2: PSS pictures for several values of the energy for the Hénon-Heiles system.

predominates but some regular regions persist (C and D). In the limit value of the energy for bounded motion (E) we have just four small regular regions that decreases slowly in size for higher values of E (but now we have unbounded admissible regions). On Fig. 2 we show the PSS pictures equivalent to the $\text{OFLI}^2_{\text{TT}}$ pictures A, C and E of Fig. 1. We show as the Poincaré sections and the chaos indicators give complementary results, but the chaos indicator points out is an easier way all the dynamical structures.

The Extensible-Pendulum problem [5] describes the movement of two parametrically coupled oscillators and it is given by the Hamiltonian

$$\mathcal{H}(q_1,\, q_2,\, p_1,\, p_2) = \frac{1}{2}\,(p_1^2 + p_2^2) + \frac{1}{2}\big((1-c)\,q_1^2 + q_2^2 - c\,q_1^2\,q_2\big),$$

and the differential system

$$\begin{aligned} \dot{q}_1 &= p_1, \qquad & \dot{p}_1 &= (c-1)\,q_1 + c\,q_1\,q_2, \\ \dot{q}_2 &= p_2, \qquad & \dot{p}_2 &= -q_2 + c\,q_1^2/2. \end{aligned}$$

The parameter c is a non-dimensional parameter defined as $c := 1 - m\mathrm{g}/kl = 1 - (\omega_p/\omega_s)^2$, being m the mass of the pending object, g the gravity acceleration, l the length of the

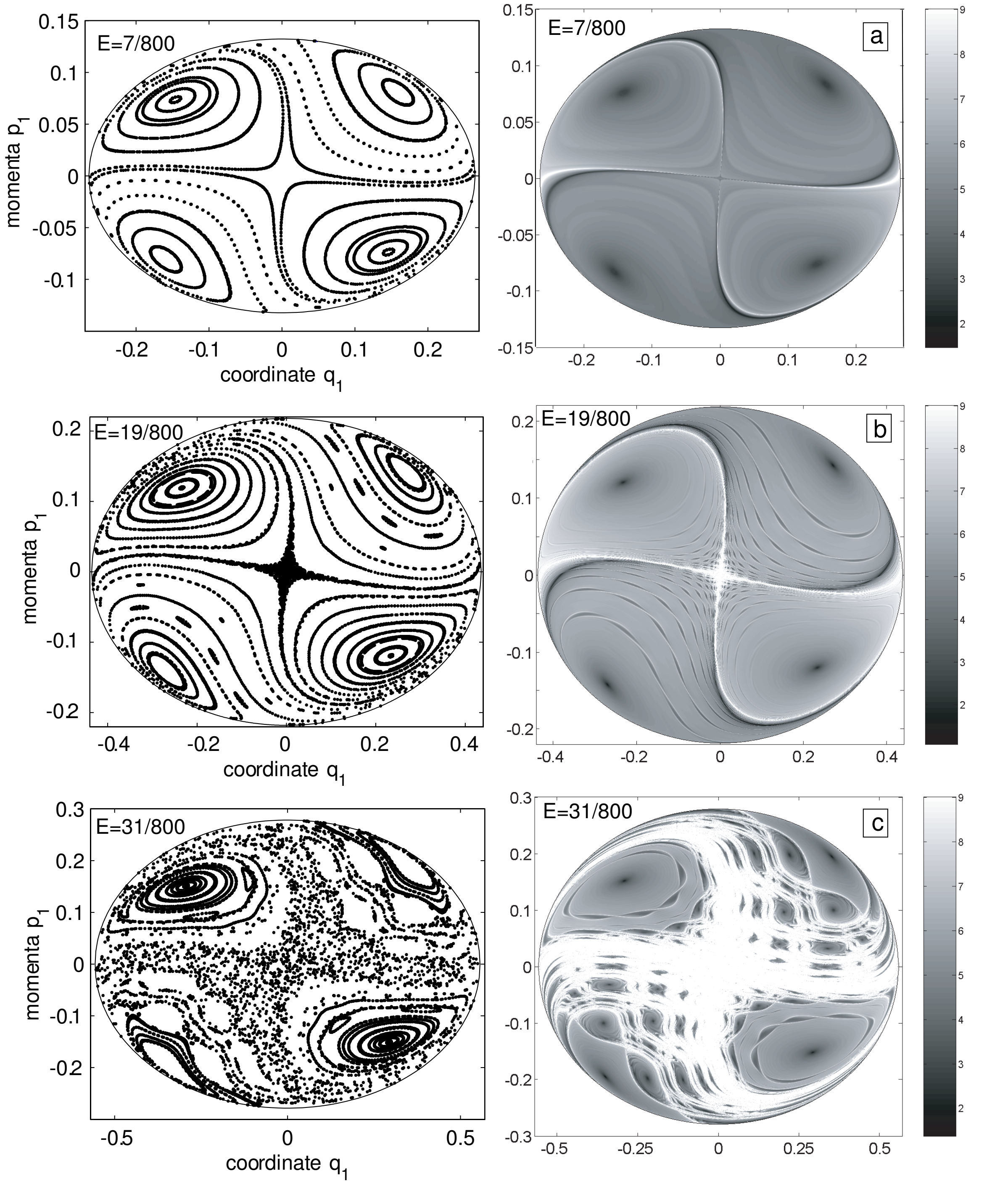

Figure 3: PSS (left) and $\mathrm{OFLI}^2_{\mathrm{TT}}$ (right) pictures for several values of the energy for the Extensible-Pendulum problem.

spring at equilibrium under a static load $m\mathrm{g}$, ω_p and ω_s are the small oscillation frequencies of the spring and pendulum, respectively. Note that $\omega_p \leq \omega_s$, and so $c \in [0,\, 1]$.

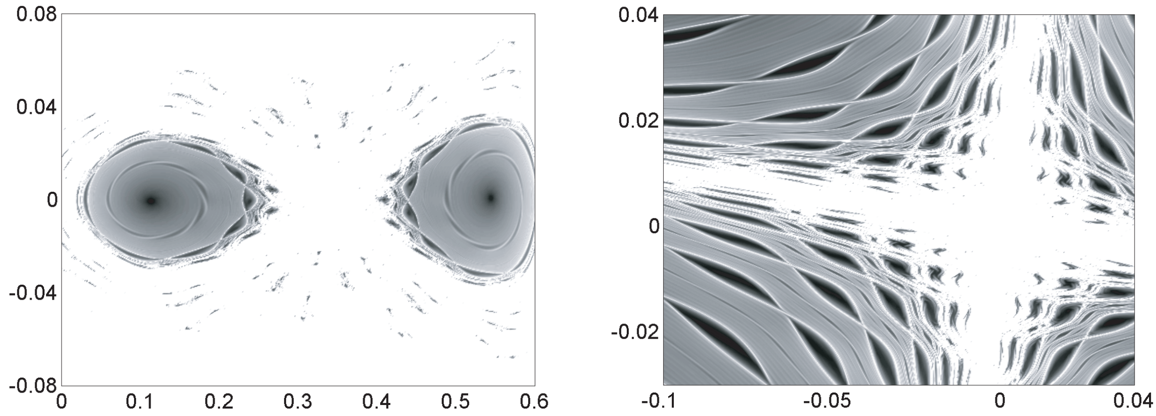

Figure 4: Left: magnification of the E picture of the $\mathrm{OFLI}^2_{\mathrm{TT}}$ plot of Fig. 1. Right: magnification of the 'b' picture of the $\mathrm{OFLI}^2_{\mathrm{TT}}$ plot of Fig. 3.

On Fig. 3 on the left we show the PSS, taking $q_2 = 0$ and obtaining p_2 from the energy value, for the values of the energy $E = 7/800$, $19/800$ and $31/800$ and taking $c = 0.75$ for the pictures 'a', 'b' and 'c' respectively. From the figures we observe as when the energy grows the chaotic region increases its size. On Fig. 3 on the right we show the $\mathrm{OFLI}^2_{\mathrm{TT}}$ counterpart up to the final time $t_f = 600$. Again, the $\mathrm{OFLI}^2_{\mathrm{TT}}$ locates without any effort the separatrices, the chain islands, and so on. Comparing the PSS and $\mathrm{OFLI}^2_{\mathrm{TT}}$ pictures we note how the chaos indicator gives a much better analysis, in an automatic way, when both regular and chaotic motions appear.

On Fig. 4 on the left we show the magnification of the region $y \times Y \in [0, 0.6] \times [-0.08, 0.08]$ for the Hénon-Heiles system, revealing the chain islands around the remaining KAM tori. On the right we show the magnification of the region $q_1 \times p_1 \in [-0.1, 0.04] \times [-0.03, 0.04]$ for the Extensible-Pendulum problem.

Besides, on Fig. 5, we present, for the Hénon-Heiles problem, a parametric evolution y vs. Energy E taking $Y = 0$ (we note that this picture is not possible to obtain with the PSS). This picture gives a detailed diagram of the evolution of the dynamical system when the parameter E changes. We observe as when the energy is low the system is highly regular. When E reaches a value near $E = 0.1486$ a period doubling bifurcation appears, changing the character of the equilibrium points. For high values of the energy the dynamical behavior is highly complicated, appearing large chaotic regions.

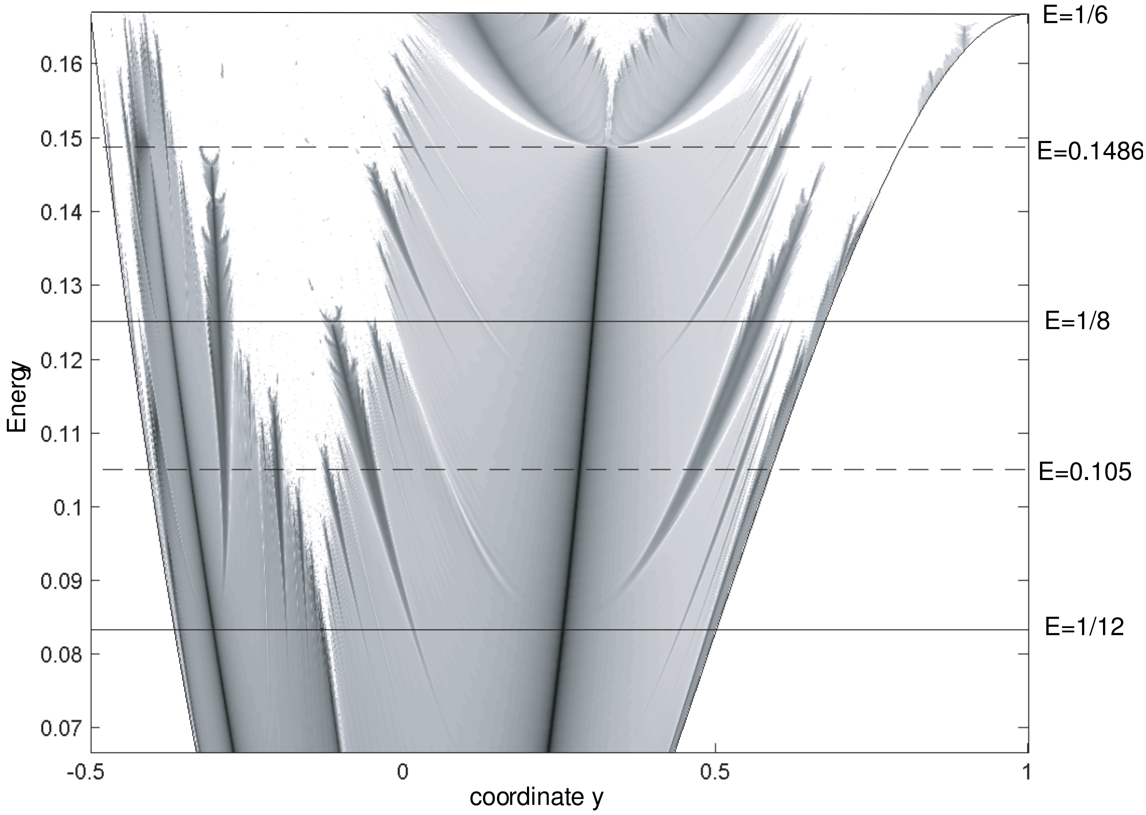

Figure 5: Parametric evolution (coordinate y vs. energy E) of the $\mathrm{OFLI}^2_{\mathrm{TT}}$ for the Hénon-Heiles system.

4 Conclusions

In this paper we review some aspects of the $\mathrm{OFLI}^2_{\mathrm{TT}}$ chaos indicator in analyzing dynamical systems. These plots permit to complement the counterpart PSS adding new features. Moreover, these techniques allow us to obtain pictures that show the evolution depending parameters, pictures that a standard PSS techniques cannot obtain. The use of second order variational equations is the main advantage and drawback of the $\mathrm{OFLI}^2_{\mathrm{TT}}$, advantage because is the first indicator that uses them and permits faster and sharper results and drawback due to the process of generating the equations that in some cases may be cumbersome. This disadvantage is eliminated by using a recently proposed modified Taylor scheme [3], that permits to avoid the determination and programming of any variational equation.

Acknowledgments

The author has been supported by the Spanish Research Grant DGYCT BFM2003-02137.

References

[1] Barrio, R. [2005] "Performance of the Taylor series method for ODEs/DAEs," *Appl. Math. Comput.* **163**, 525–545.

[2] Barrio, R. [2005b] "Sensitivity Tools vs. Poincaré Sections," *Chaos Solitons Fractals* **25**, 711–726.

[3] Barrio, R. [2006] "Sensitivity analysis of ODEs/DAEs using the Taylor series method," *SIAM J. Sci. Comput.* **27**, 1929–1947.

[4] Barrio, R., Blesa, F. & Lara, M. [2005] "VSVO formulation of Taylor methods for the numerical solution of ODEs," *Comput. Math. Appl.* **50**, 93–111.

[5] Carretero-González, R., Núñez-Yépez, H.N. & Salas-Brito, A.L. [1994] "Regular and chaotic behaviour in extensible pendulum," *Eur. J. Phys.* **15**, 139–148.

[6] Cincotta. P.M., Giordano, C.M. & Simó, C. [2003] "Phase space structure of multi-dimensional systems by means of the mean exponential growth factor of nearby orbits," *Phys. D* **182**, 151–178.

[7] Contopoulos, G. & Voglis, N. [1996] "Spectra of stretching numbers and helicity angles in dynamical systems," *Celes. Mech. Dyn. Astr.* **64**, 1–20.

[8] Contopoulos, G. & Voglis, N. [1997] "A fast method for distinguishing between order and chaotic orbits," *Astr. Astrophys.* **317**, 73–82.

[9] Fouchard, M., Lega, E., Froeschlé, C. & Froeschlé, C. [2002] "On the relationship between fast Lyapunov indicator and periodic orbits for continuous flows," *Celes. Mech. Dyn. Astr.* **83**, 205–222.

[10] Froeschlé, C. & Lega, E. [2000] "On the structure of symplectic mappings. The fast Lyapunov indicator: a very sensitivity tool," *Celes. Mech. Dyn. Astr.* **78**, 167–195.

[11] Galias, Z. & Zgliczyński, P. [1998] "Computer assisted proof of chaos in the Lorenz equations," *Phys. D* **115**, 165–188.

[12] Guzzo, M., Lega, E. & Froeschlé, C. [2002] "On the numerical detection of the effective stability of chaotic motions in quasi-integrable systems," *Phys. D* **163**, 1–25.

[13] Hénon, M. & Heiles, C. [1964] "The applicability of the third integral of motion: some numerical experiments," *Astron. J.* **1**, 73–79.

[14] Hairer, E. and Hairer, M. [2003] "GniCodes—Matlab programs for geometric numerical integration," in *Frontiers in numerical analysis* (Springer-Verlag, Berlin) pp. 199–240.

[15] Laskar, J. [1990] "The chaotic motion of the solar system: a numerical estimate of the size of the chaotic zones," *Icarus* **88**, 266–291.

[16] Laskar, J. [1993] "Frequency analysis for multi-dimensional systems. Global dynamics and diffusion," *Phys. D* **67**, 257–281.

[17] Skokos, Ch. [2001] "Aligment indices: a new, simple method for determining the ordered or chaotic nature of orbits," *J. Phys. A: Math. Gen.* **34**, 10029–10043.

[18] Skokos, Ch., Antonopoulos, Ch., Bountis, T.C. & Vrahatis, M.N. [2004] "Detecting order and chaos in Hamiltonian systems by the SALI method," *J. Phys. A: Math. Gen.* **37**, 6269–6284.